MAGNETIC FIELD FINITE ELEMENT MODELING OF MAGNETIC BEARINGS INCLUDING ROTOR MOTION EFFECTS AND EDDY CURRENTS

R. D. Rockwell, Jr.
P. E. Allaire
Mechanical, Aero & Nuclear Engineering
U. of Virginia
Charlottesville, VA
USA

J. C. Heinrich
Aero & Mechanical Engineering
U. of Arizona, Tucson, AZ, USA

G. K. Foshage
Honeywell, Inc.
Phoenix, AZ, USA

ABSTRACT

The purpose of this paper is to develop the finite element model of magnetic and electric fields in magnetic bearings, including the motion of the magnetic material in the rotor. A good computational model is of importance in calculating the magnetic field, forces on the rotor and in determining eddy current losses.

INTRODUCTION

Sarma [1] derived a magnetic vector potential, A, and an electric vector potential, ϕ, for non-linear, time dependent electromagnetic field problems but without considering motion of the magnetic material. Muramatsu, et al. [2] considered a set of coupled vector differential equations for A and ϕ in fixed and moving coordinate systems for eddy current analysis in moving conductors. Chan and Williamson [3] considered the analysis of eddy current problems involving relative motion. They also obtained a coupled differential equation for A and ϕ in three dimensions. Ito, et al. [4] developed a time dependent differential equation for A including traveling magnetic field effects (motional effects) which is uncoupled from ϕ but involves the curl of the vector magnetic potential. Numerical instabilities arise at high velocities and a method of upwinding is required to remove the instability [3,4].

Eddy current losses in magnetic bearings were first calculated using a finite element model by Yoshimoto [5]. He assumed a sinusoidal rotational current distribution for a two dimensional magnetic bearing in terms of a vector magnetic potential. Matsumura, et al. [6] presented a Fourier analysis of the distribution of the magnetic field in a magnetic bearing. Kasarda, et al. [7,8] have presented experimental results on eddy currents and employed predictions of eddy currents based upon classical power loss formulas developed for transformers and electric motors using an effective frequency based upon the number of poles in the bearing.

The present approach starts with Maxwell's equations and develops an uncoupled form of the governing differential equation for the magnetic vector potential. The eddy current flow is then evaluated separately. Only two dimensional equations are treated in this paper.

MAGNETIC POTENTIAL FORMULATION

The equations for the magnetic and electric field in a magnetic bearing are solved in a stator fixed coordinate system so they are not time dependent. Maxwell's equations and linear material relations for the magnetic flux density, B, the electric field, E, the magnetic field, H, and current density, J, with the magnetic reluctivity ν and the conductivity σ are

$$\nabla \cdot \bar{B} = 0 \quad , \quad \nabla X \bar{H} = \bar{J}$$
$$\nabla X E = \nabla X (\bar{U} X \bar{B}) \qquad (1)$$
$$\bar{J} = \sigma \bar{E} \quad , \quad \bar{H} = \nu \bar{B}$$

Here Faraday's law includes the rotor magnetic material moving with velocity U relative to the stator fixed coordinate system. The magnetic vector potential A is defined by the equation

$\bar{B} = \nabla X \bar{A}$ which satisfies $\nabla \cdot \bar{B} = 0$.

In Ampere's law, the current density on the right hand side is split into a known coil current density, J_s, defined in the coil volume, and an unknown eddy current density, J_e defined in the remaining bearing analysis volume.

Faraday's law can be written as the curl of a vector quantity which equals zero. Thus it can be expressed as the gradient of an electric scalar potential, ϕ. The eddy current expression can now be expressed as

$$\bar{J}_e = \sigma[-\nabla\phi + \bar{U}X(\nabla X\bar{A})] \qquad (2)$$

Ampere's law becomes

$$\nu\nabla X(\nabla X\bar{A}) + \sigma\nabla\phi - \sigma\bar{U}X(\nabla X\bar{A}) = \bar{J}_s \qquad (3)$$

Defining the gauge of Maxwell's equations as

$$\nu\nabla\cdot(\bar{A}) + \sigma\phi = 0 \qquad (4)$$

and using a vector identity, Ampere's law is transformed to

$$\nu\nabla\cdot\nabla\bar{A} + \sigma\bar{U}X(\nabla X\bar{A}) = -\bar{J}_s \qquad (5)$$

as simplified from [9]. This is a suitable form for solution using finite elements.

TWO DIMENSIONAL FINITE ELEMENT FORMULATION

In two dimensions, the governing differential equation for the axial component of the magnetic vector potential, A_z, is obtained from the z component of (5) with the velocity terms included as

$$\nu\frac{\partial^2 A_z}{\partial x^2} + \nu\frac{\partial^2 A_z}{\partial y^2} - \sigma_z U_x\frac{\partial A_z}{\partial x} - \sigma_z U_y\frac{\partial A_z}{\partial y} + J_{sz} = 0 \qquad (6)$$

This equation applies to the case of a solid rotor (not laminated) so that eddy currents are free to propagate in the axial (z) direction. The magnetic vector potential equation is similar to the 2-D diffusion-convection equation in fluid mechanics. Then the rotor motion terms are modeled using upwinding methods developed in the fluid mechanics area of research. Let the finite element approximation to the solution be A*, then the two dimensional differential equation has the form

$$\nu\frac{\partial^2 A_z^*}{\partial x^2} + \nu\frac{\partial^2 A_z^*}{\partial y^2} - \sigma_z U_x\frac{\partial A_z^*}{\partial x} - \sigma_z U_y\frac{\partial A_z^*}{\partial y} + J_{sz} = \epsilon_A(x,y) \qquad (7)$$

where $\epsilon_A(x,y)$ is the error [10]. The weighted residual for each element then has the form

$$\{R_n^e\} = -\int_{A^e}\{W_n^e\}\,\epsilon_A^e\,dA^e \qquad (8)$$

where A^e is the element area and n has the values 1,2,3,4 for a four node isoparametric element. The weighting functions are written as

$$\{W_{zn}\} = \{G_n\}^T + \frac{\beta_z\bar{h}_z}{2U_{mz}}\{U_x\}[D_G]^T \qquad (9)$$

where G_n are the finite element shape functions, U_x are the rotor velocity components, and D_G is the matrix of the derivatives of the shape functions. The second term on the right provides the upwinding terms, adapted from computational fluids [11,12] necessary for the

motion terms in the rotor. In this analysis, the second term is actually only employed for the velocity terms, as is customary in finite elements for computational fluids.

MAGNETIC BEARING APPLICATION

Magnetic field results have been obtained for a typical magnetic bearing including rotor motion effects. Figure 1 shows the magnetic bearing geometry considered here and Fig. 2 shows the finite element mesh. The mesh employed 4480 elements and 4640 nodes.

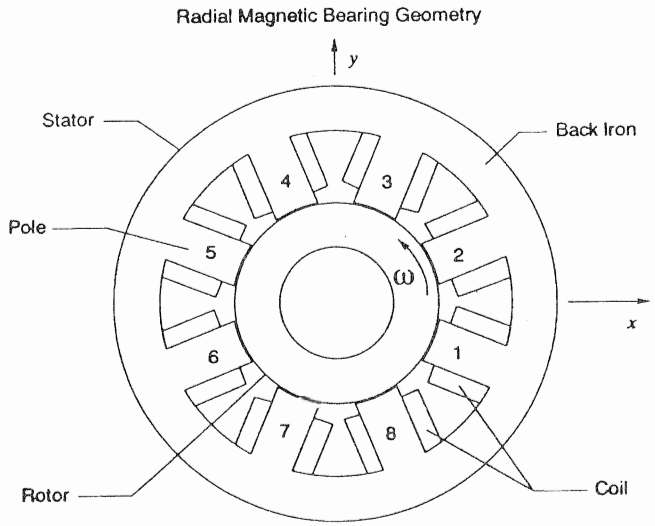

Figure 1. Magnetic Bearing Geometry

The bearing has 8 poles, rotor OD = 90.9 mm (3.58 in), shaft OD = 50.8 mm (2.0 in), stator OD = 196.2 mm (7.726 in), axial length of bearing L = 43.6 mm (1.715 in) (without coils), and air gap = 0.762 mm (0.030 in). The radial length of each leg is 31.8 mm (1.253 in) and the circumferential width of each leg is 21.1 mm (0.79 in). The conductivity of the rotor is 1.03×10^7 1/Ωm in the axial direction and the relative permeability of the rotor and stator material is 3,000.

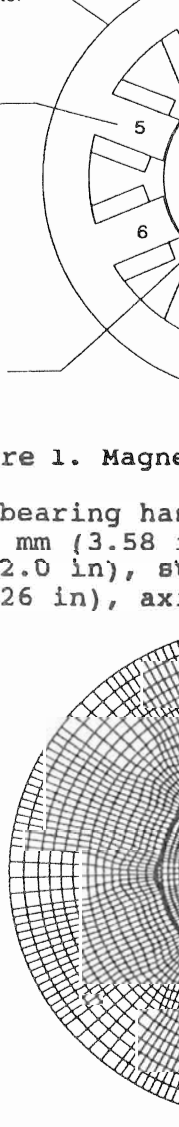

Figure 2. Finite Element Mesh

The calculated magnetic vector potential has been obtained for the case where only two poles (1 and 2) are activated with NI = 420 amp-turns. The value of A_z is then plotted along the rotor surface at 0 rpm in Fig. 3. Fig. 4 shows A_z for 9,550 rpm (1000 rad/s)

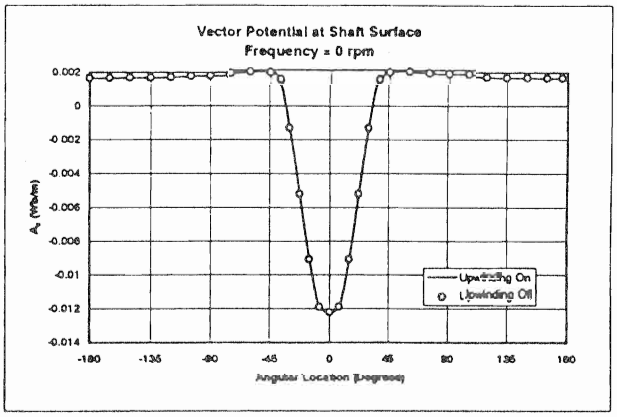

Figure 3. Magnetic Vector Potential, A_z, At Rotor Surface For 0 rpm

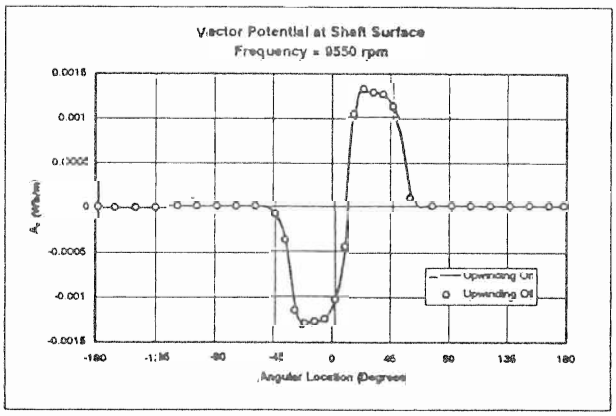

Figure 4. Magnetic Vector Potential, A_z, At Rotor Surface For 9,550 rpm

indicating the shift of the peaks in the direction of motion of the rotor. The values are shown both with upwinding off and upwinding on. In this analysis, the effect of upwinding is found to be not very important.

Magnetic flux lines for 0 rpm are shown in Fig. 5. As the rotor rotational velocity increases, the flux lines shift in the direction of the velocity. Fig. 6 shows the lines of magnetic flux for 95.5 rpm.

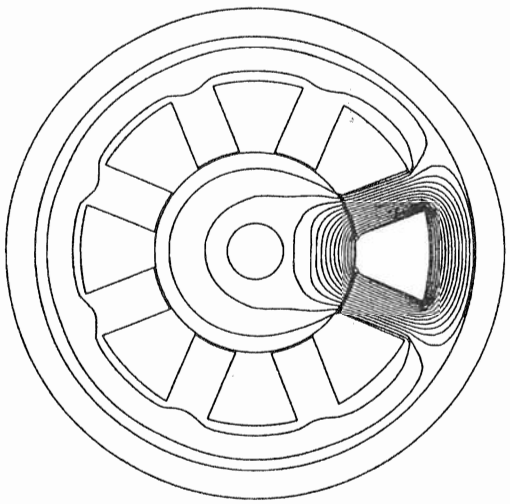

Figure 5. Magnetic Flux Lines In Magnetic Bearing At 0 rpm

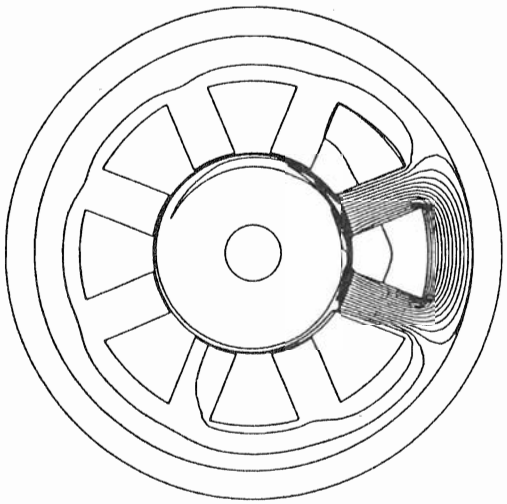

Figure 6. Magnetic Flux Lines In Magnetic Bearing At 95.5 rpm

Fig. 7 shows the result at 950 rpm. Note that the eddy current effects under the edge of each pole induce magnetic flux in the adjacent pole on the direction opposite to the motion. Fig. 8 plots the magnetic flux lines at 9,550 rpm, which further illustrates this effect. All of the plots in Figs. 5-8 have upwinding on.

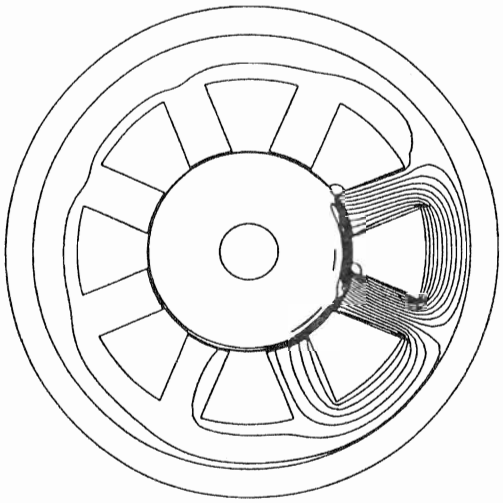

Figure 7. Magnetic Flux Lines In Magnetic Bearing At 955 rpm

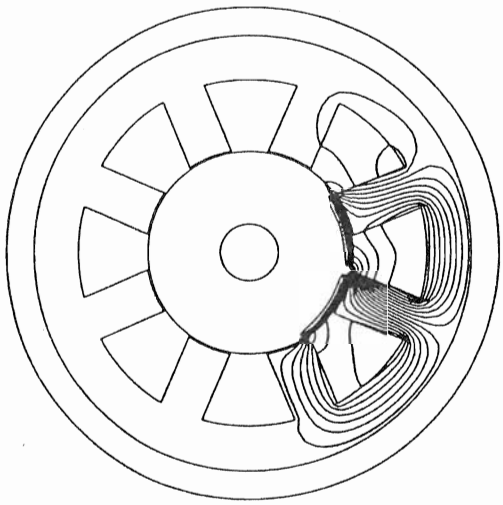

Figure 8. Magnetic Flux Lines In Magnetic Bearing At 9,550 rpm

The x and y force components are calculated using the Maxwell stress tensor for the forces. The results are given in Fig. 9. As the rotational speed increases, large eddy currents are set up in the unlaminated rotor. These in turn develop flux in the air gap which opposes the applied flux. The applied force on the rotor decreases to zero.

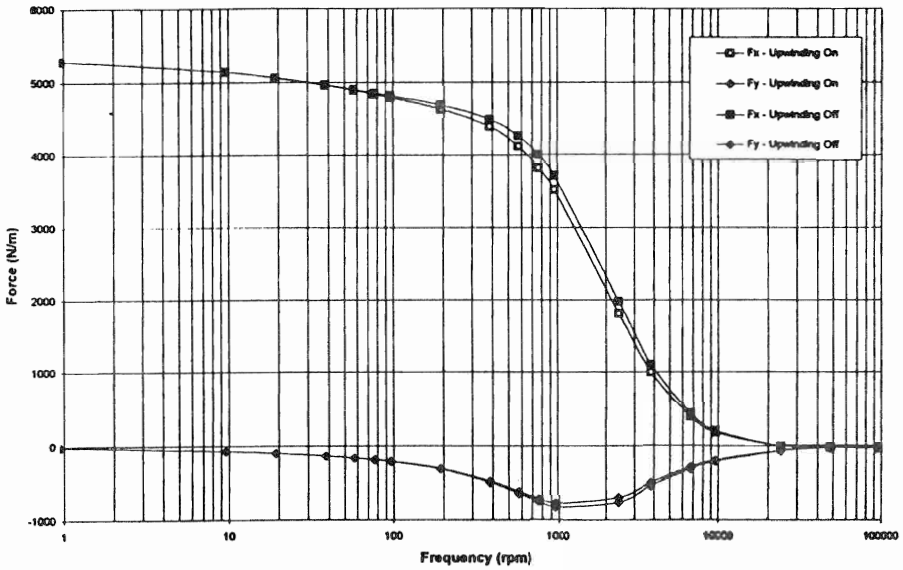

Figure 9. Forces Acting On Rotor vs. Rotational Speed

EDDY CURRENTS

The eddy currents in the rotor are evaluated from

$$J_{ze} = \sigma_z U_x \frac{\partial A_z}{\partial x} + \sigma_z U_y \frac{\partial A_z}{\partial y} \quad (10)$$

Figs. 10 and 11 show the eddy current patterns in the rotor for 955 rpm and 9,550 rpm.

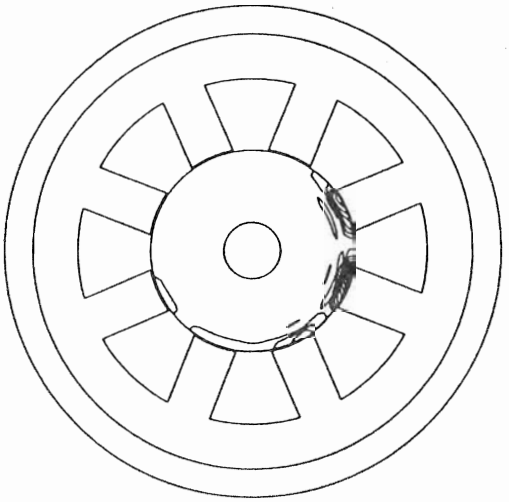

Figure 10. Eddy Current Density In Magnetic Bearing At 955 rpm

Both Figs. 10 and 11 illustrate the formation of eddy currents under each pole edge, including the upstream edge of pole 1. The power loss for the full rotor is shown in Fig. 12. It increases substantially up to a peak value and then levels

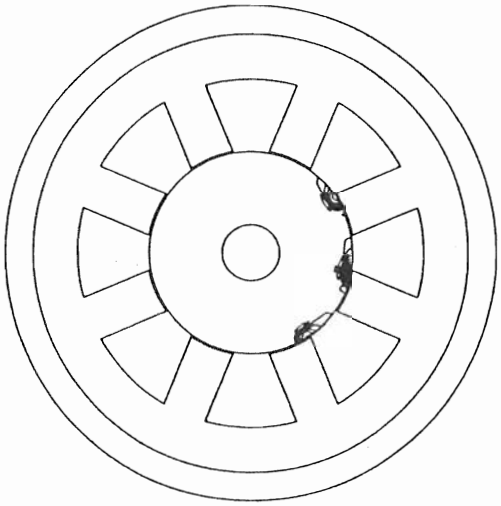

Figure 11. Eddy Current Density In Magnetic Bearing At 9550 rpm

off at the maximum value. All of the coil energy goes into producing eddy currents and no levitating force on the rotor is obtained.

CONCLUSIONS

A general differential equation for the magnetic vector potential has been derived for a magnetic bearing geometry. Unlike previous works [2,3], an uncoupled equation for A is derived and the eddy current evaluation is a secondary calculation. An upwinded finite element solution method has been formulated although upwinding did not prove to be much of a factor in this particular analysis, due to

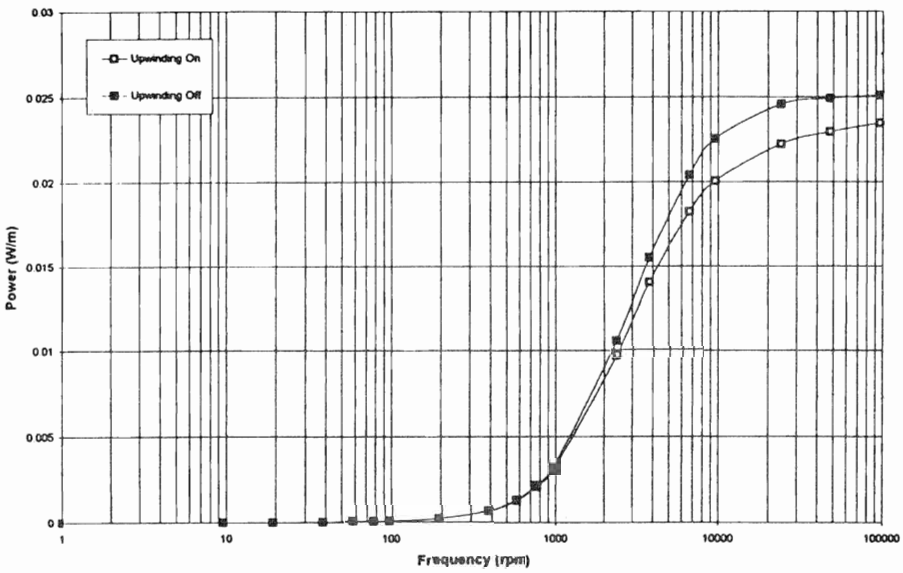

Figure 12. Rotor Power Loss Due to Eddy Currents vs. Rotor Speed

the use of a full bearing model (360 degrees), rather than a partial model. An example two dimensional radial bearing with a solid rotor was evaluated using finite elements.

REFERENCES

1. Sarma, M. S., "Potential Functions in Electromagnetic Field Problems," IEEE Trans. on Magnetics, Vol. MAG-6, No. 3, September, 1970, pp. 513-518.

2. Muramatsu, K., Nakata, T., Takahashi, N., and Fujiwara, K., "Comparison of Coordinate Systems for Eddy Current Analysis in Moving Conductors," IEEE Trans. on Magnetics, Vol 28., No. 2, 1992, pp. 1186-1189.

3. Chan, E. K. C., and Williamson, S., "Factors Influencing the Need for Upwinding in Two Dimensional Field Calculations," IEEE Trans. on Magnetics, Vol. 28, No. 2, 1992, pp. 1611-1614.

4. Ito, M., Takahashi, T., and Odamura, M., "Up-Wind Finite Element Solution of Traveling Magnetic Field Problem," IEEE Trans. on Magnetics, Vol. 28, No. 2, 1992, pp. 1605-1610.

5. Yoshimoto, T., "Eddy Current Effect in Magnetic Bearing Model," IEEE Transactions on Magnetics, Vol. Mag-19, September 1983.

6. Matsumura, F., Fujita, M., and Ozaki, Y., "Characteristics of Friction on Magnetic Bearings," Trans. IEE of Japan, 108-D, No. 5, 1988, pp. 462-468.

7. Kasarda, M. E. F., Allaire, P. E., Hope, R. W., and Humphris, R. R., "Measured and Predicted Losses in Planar Radial Bearings, Proceedings of MAG '93, Alexandria, VA, July 1993.

8. Kasarda, M. E. F., and Allaire, P. E., "Experimentally Measured and Improved Calculated Losses in Planar Radial Magnetic Bearings," Accepted for Publication, STLE, 1996.

9. Allaire, P. E., Rockwell, R. D., Rowe, J., and Kasarda, M. E. F., "Magnetic and Electric Field Equations for Magnetic Bearing Applications", Transactions of MAG '95, Technomics Publishing, 1995.

10. Allaire, P. E., Basics of the Finite Element Method, W. C. Brown (distributed by West Publishing), 1985.

11. Heinrich, J. C., and Yu, C. C., 1988, "Finite Element Simulations of Buoyancy-Driven Flows with Emphasis on Natural Convection in a Horizontal Circular Cylinder," Computational Methods of Applied Mechanics in Engineering, Vol. 69, pp. 1-27.

12. Pepper, D. W. and Henrich, J. C., The Finite Element Method: Basic Concepts and Applications, Hemisphere Publishing, 1992.

ACKNOWLEDGEMENT

Partial funding for this work was provided by NASA Lewis Research Center.